Astron. Astrophys. 262, 501–514 (1992)

ASTRONOMY AND ASTROPHYSICS

Accelerated complete-linearization method for calculating NLTE model stellar atmospheres

I. Hubeny* and T. Lanz**

NASA Goddard Space Flight Center, Code 681, Greenbelt, MD 20771, USA

Received January 7, accepted March 13, 1992

Abstract. Two approaches to accelerating the method of complete linearization for calculating NLTE model stellar atmospheres are suggested. The first one, the so-called Kantorovich variant of the Newton–Raphson method, consists of keeping the Jacobi matrix of the system fixed, which allows us to calculate the costly matrix inversions only a few times and then keep them fixed during the subsequent computations. The second method is an application of the Ng acceleration. Both methods are extremely easy to implement with any model atmosphere code based on complete linearization. It is demonstrated that both methods, and especially their combination, yield a rapidly and globally convergent algorithm, which takes 2 to 5 times less computer time, depending on the model at hand and the required accuracy, than the ordinary complete linearization. Generally, the time gain is more significant for more complicated models. The methods were tested for a broad range of atmospheric parameters ($T_{\rm eff} = 10\,000$, 25 000 and 50 000 K), and in all cases they exhibited similar behavior. Ng acceleration applied on the Kantorovich variant thus offers a significant improvement of the standard complete-linearization method, and may now be used for calculating relatively involved NLTE model stellar atmospheres.

Key words: radiative transfer – stars: atmospheres – stars: early-type

1. Introduction

The method of complete linearization, first introduced by Auer & Mihalas (1969), represents a foundation on which most of the progress in stellar atmospheric modeling made during the last two decades was based. Until recently, this was the only practical method for calculating reliable non-local-thermodynamic-equilibrium (NLTE) model atmospheres for hot ($T_{\rm eff} > 10\,000$ K) stars. As has been amply demonstrated, complete linearization is a very powerful method, yet it possesses a serious drawback: only a relatively small number of opacity sources (lines) and simple atomic models can be treated, due to the cubic increase of computer time as the number of unknowns increases.

Recently, two powerful methods have been developed which offer a substantial reduction of computer time with respect to the original complete linearization, which therefore allows one to treat more realistic model atoms in NLTE, including the effects of many lines and continua. One method, called the multi-frequency/multi-gray algorithm, was developed by Anderson (1985, 1987). The method uses an ingenious rearranging of individual frequency points into a small set of frequency blocks. Mathematically, it is still based on complete linearization. The other method is an application of the accelerated lambda iteration (ALI) technique, developed by Werner and collaborators (Werner 1986, 1987, 1989; Dreizler & Werner 1991). Model atmospheres taking into account hundreds of atomic energy levels and hundreds to thousands of transitions are now becoming possible.

Despite these new developments, the standard complete linearization remains still a viable method. Generally, while the ALI methods require much less computational effort per iteration, the number of iterations needed is typically rather large, of the order of tens to even hundreds. In contrast, complete linearization, which requires many more operations per iteration, usually exhibits much faster convergence – cases where as few as 5 iterations produce a reasonably converged model are not exceptional. Moreover, convergence with complete linearization is *global*, if it converges at all. Another conceptual advantage of complete linearization is the ease of coding it and generalizing it to more complex physical situations (for instance, treating partial frequency redistribution in line transitions does not introduce any particular complications, in contrast to the ALI methods). Finally, from the practical view, there already exist several user-friendly and well-documented computer programs based on complete linearization (Mihalas et al. 1975; Hubeny 1988), which are currently being used worldwide for various modeling purposes.

For all these reasons it is highly desirable to seek out modifications and improvements of complete linearization which would preserve its favorable properties, particularly the rapid and global convergence, while reducing as much as possible the computational effort per iteration and the number of iterations required. It is the aim of the present paper to suggest two such improvements, and to demonstrate that they indeed lead to a dramatic reduction of computer time in practically all cases of hot star atmospheric modeling.

Send offprint requests to: I. Hubeny
* Universities Space Research Association (USRA)
** NRC-NASA Research Associate

2. The formulation

2.1. Ordinary complete linearization

The problem of constructing a model atmosphere consists in solving simultaneously the set of structural equations describing the physical state of a stellar atmosphere. We limit ourselves here to the so-called classical stellar atmosphere problem, although the subsequent development may be applied to more general situations. Assuming a plane-parallel, horizontally homogeneous atmosphere in hydrostatic, radiative, and statistical equilibrium, the basic set of equations to be solved consists of the radiative transfer equations for a selected set of frequency points, the hydrostatic equilibrium equation, the radiative equilibrium equation, and the set of statistical equilibrium equations for chosen atomic energy levels. The equations are discretized in frequency and depth, which yields a set of highly coupled, non-linear algebraic equations.

Within these approximations, the physical state of an atmosphere may then be fully described by a set of vectors ψ_d for every depth point d, $d=1, \ldots,$ ND, ND being the total number of depth points. The (column) vector ψ_d is given by

$$\psi_d=\{J_1, \ldots, J_{\mathrm{NF}}, N, T, n_e, n_1, \ldots, n_{\mathrm{NL}}\}^{\mathrm{T}}, \tag{1}$$

where J_i is the mean intensity of radiation in the ith frequency point, N the total particle number density, T the temperature, n_e the electron density, and n_i the atomic level populations; we have omitted the depth subscript d. The dimension of vector ψ_d is NN, NN = NF + NL + 3, NF is the number of frequency points, and NL number of atomic energy levels. Superscript T means the transposition, and should not be confused with temperature. Strictly speaking, vector ψ_d should contain specific intensities of radiation, $I(\nu_i, \mu_j)$, (μ_j being discretized values of the directional cosines), instead of mean intensities $J(\nu_i)$. However, thanks to the variable Eddington factor technique, a simplified form [Eq. (1)] may be used. This point will be further discussed in Sect. 2.2.

The set of structural equations may be written formally as

$$\boldsymbol{P}(\boldsymbol{x})=0, \tag{2}$$

where $\boldsymbol{x}$ is a column vector formed from all column vectors ψ_d,

$$\boldsymbol{x}=\{\psi_1^{\mathrm{T}}, \ldots, \psi_{\mathrm{ND}}^{\mathrm{T}}\}^{\mathrm{T}},$$

its dimension is therefore NN × ND, and $\boldsymbol{P}$ is a non-linear operator,

$$\boldsymbol{P}=\{\boldsymbol{P}_1, \ldots, \boldsymbol{P}_{\mathrm{ND}}\}^{\mathrm{T}}, \tag{3}$$

and

$$\boldsymbol{P}_d=\{P_1, \ldots, P_{\mathrm{NF}}, P_{\mathrm{NF}+1}, \ldots, P_{\mathrm{NN}}\}^{\mathrm{T}}, \tag{4}$$

where the first NF equations are the discretized radiative transfer equations at depth d, the (NF + 1)th equation is the hydrostatic equilibrium at this depth, and so on.

The original complete linearization is nothing more than the Newton–Raphson (sometimes also called Newton–Kantorovich) method of solving Eq. (2), namely

$$J(\boldsymbol{x}^{(n)})\delta\boldsymbol{x}^{(n)}=-\boldsymbol{P}(\boldsymbol{x}^{(n)}), \tag{5a}$$

or, equivalently,

$$\boldsymbol{x}^{(n+1)}=\boldsymbol{x}^{(n)}-J(\boldsymbol{x}^{(n)})^{-1}\boldsymbol{P}(\boldsymbol{x}^{(n)}), \tag{5b}$$

where J is the Jacobi matrix (Jacobian),

$$J_{ij}=\frac{\partial P_i}{\partial x_j}. \tag{6}$$

Since the system [Eq. (2)] represents a *finite difference* solution of at most second-order differential equations (i.e. the Feautrier form of the transfer equation; see, for example, Mihalas 1978), the Jacobian J has a particularly simple structure, namely a block-tridiagonal form, and Eq. (2) is traditionally written (Mihalas 1978) as

$$-A_d^{(n)}\delta\psi_{d-1}^{(n)}+B_d^{(n)}\delta\psi_d^{(n)}-C_d^{(n)}\delta\psi_{d+1}^{(n)}=\boldsymbol{L}_d^{(n)}, \tag{7}$$

which now also indicates the explicit dependence of the matrices on the iteration number n. Here A, B, C are NN × NN matrices, and $\boldsymbol{L}_d^{(n)}=\boldsymbol{P}_d(\boldsymbol{x}^{(n)})$ is the residuum vector (of dimension NN) at depth d.

Since the Jacobian is of a block-tridiagonal form, its inversion in Eq. (5) is not performed explicitly (otherwise one would be faced with the inversion of a matrix typically $10^4 \times 10^4$ even for simple model atmospheres, which is clearly out of the question even for the fastest available computers). Instead, Eq. (5) is solved by applying a block-Gaussian elimination procedure. One first constructs auxiliary NN × NN matrices D_d and vectors v_d of dimension NN by the recurrence relations (here we omit the superscript n)

$$D_d=(B_d-A_dD_{d-1})^{-1}C_d, \quad D_1=B_1^{-1}C_1, \tag{8a}$$

$$v_d=(B_d-A_dD_{d-1})^{-1}(\boldsymbol{L}_d+A_dv_{d-1}), \quad v_1=B_1^{-1}\boldsymbol{L}_1, \tag{8b}$$

and the solution is found by a "back-substitution",

$$\delta\psi_d=D_d\delta\psi_{d+1}+v_d, \quad \delta\psi_{\mathrm{ND}+1}=0. \tag{9}$$

Each iteration of the complete linearization thus consists of:

(i) setting up matrices A, B, C, and the r.h.s. vectors $\boldsymbol{L}$;

(ii) calculating auxiliary matrices D and vectors v, Eqs. (8a) and 8b);

(iii) back-substitution, Eq. (9).

Step (ii), which involves ND inversions of (NN × NN) matrices, plus ND multiplications of two (NN × NN) matrices is usually the most time-consuming part of the model construction. (Matrix C has a special structure, so that the multiplication is much less time-consuming than the case of multiplying two full matrices.) Step (i) is typically much faster, although for very involved model atmospheres it may consume an appreciable fraction of the total time. Steps (iii), which involves only multiplication of a matrix with a vector, is very fast. Since the auxiliary matrices, D, have to be stored on an external storage medium, the computer time for this step is usually I/O-dominated.

We stress that besides steps (i)–(iii), one usually has to perform a formal solution step, which is basically a set of calculations between successive linearization iterations whose purpose is to provide consistent values of radiation intensities and level populations. To this end, one either performs several lambda iterations, or, better still, performs several sets of the equivalent-two-level atom procedures (for details, refer to Hubeny 1988). As discussed by Hubeny (1981, 1988), this step is often the decisive one in achieving convergence.

Altogether, the total computer time for the ordinary complete linearization scales roughly as

$$N_{\mathrm{iter}} \times \mathrm{ND} \times \mathrm{NN}^3.$$

Generally, one may reduce the total time either by reducing the time per iteration, or by reducing the number of iterations needed

to achieve a certain accuracy, or both. The former possibility is discussed in the following two sections, while the latter one is considered in Sect. 2.4.

2.2. *Acceleration by reducing the size of matrices*

One obvious way of reducing the computer time is to reduce the size of matrices to be inverted, i.e. to minimize NN as much as possible. Of course, this may be accomplished by reducing the complexity of the physical problem, but we exclude this here since our goal is to develop a method which handles a *given* physical problem, of arbitrary complexity, as efficiently as possible.

The reduction of NN may also be achieved by means of linearizing the system with respect to fewer quantities than the actual number of unknowns, either by linearizing only some appropriately chosen *averaged* quantities, or by keeping certain quantities *fixed* during linearization and recalculating them after a completed iteration (basically by means of a formal solution of the appropriate equation). A typical example of the first approach is the *variable-Eddington-factor technique* (VEFT; Auer & Mihalas 1970), which consists of linearizing only the (angle-averaged) mean intensities, instead of the angle-dependent specific intensities. The angular dependence of the radiation intensity then enters the formalism only through the ratios of moments, called Eddington factors. These factors are calculated before entering a linearization step, are held fixed during linearization, and are updated after a completed iteration of complete linearization by means of a frequency-by-frequency formal solution of the radiative transfer equation. This leads to an enormous saving of computer time, because NN should actually be given as $NN = NF \times NA + NL + 3$, NA being the number of angles. This means that if $NF \gg NL$ (a typical case in stellar atmospheric modeling), and $NA = 3$ (a reasonable minimum acceptable value), the computer time using VEFT is asymptotically 27 times faster! Another method of this category is the multi-frequency/multi-gray algorithm of Anderson (1985, 1987), which uses an analogy of VEFT by averaging the mean intensity of radiation over carefully constructed frequency blocks.

The latter way of reducing NN is accomplished by keeping selected radiative transition rates fixed (Hubeny 1988). These fixed rates are calculated essentially exactly in the formal solution step, are held fixed during linearization, and subsequently are updated in the next formal solution step (their treatment thus differs from what is usually understood as "fixed" transitions, by other authors, e.g. Auer et al. 1972, or Carlsson 1986, where the fixed rates are inherently approximate).

All these methods generally slow down the convergence rate. It is well known that the pure Newton–Raphson method (i.e. linearizing with respect to *all* unknowns) converges *quadratically*, if it converges at all. In adopting either technique mentioned above the quadratic convergence property is destroyed, but the corresponding increase in number of iterations needed (usually moderate) is more than outweighed by the dramatic decrease of computer time per iteration. In the following, we shall refer to these techniques as the *lagging techniques*, or simply "lagging".

2.3. *Acceleration by avoiding repeated matrix inversions*

There is a whole class of methods of solving a system of non-linear equations other than the standard Newton–Raphson technique. In the context of model stellar atmospheres, one such method was recently employed by the Kiel group (Hamann et al. 1991; Dreizler & Werner 1991). They used a variant of the quasi-Newton method (Broyden 1965; Schubert 1970; for a review see, for instance, Wait 1979), which represents a multidimensional extension of the secant method.

Other possibilities, not yet tested in the context of stellar atmospheres, include the non-linear Jacobi method (replacing the exact Jacobian by its diagonal), or gradient methods, where the corrections are obtained by multiplying the residuum vector by the transposed Jacobian (Wait 1979).

A straightforward modification of the standard Newton–Raphson method, sometimes called Kantorovich method, is to keep the Jacobian fixed,

$$\boldsymbol{x}^{(n+1)} = \boldsymbol{x}^{(n)} - J(\boldsymbol{X})^{-1}\boldsymbol{P}(\boldsymbol{x}^{(n)}), \tag{10}$$

where $\boldsymbol{X}$ is a fixed value, usually taken as some $\boldsymbol{x}^{(k)}$, $k < n$. In this case, one calculates the matrix inversion only once, and the fixed inverse matrix is used in all subsequent iterations. Obviously, if $J(\boldsymbol{x}^{(n)})$ is significantly different from $J(\boldsymbol{X})$, convergence can be slow or can fail altogether (see Kantorovich 1949, or Kantorovich & Akilov 1964). A sensible strategy is therefore to first perform several ordinary Newton–Raphson iterations, and, when one is already close to a converged solution, switch to the Kantorovich variant, Eq. (10).

Surprisingly, this method has never been applied to the problem of stellar atmospheres. A likely reason is that most workers who have used the complete-linearization method since the time of its introduction experience ubiquitous convergence problems even with the standard variant. They might have been reluctant to try something which may potentially spoil an already very fragile convergence.

In line with our stated goal, we have tested this method extensively and have found that it works surprisingly well; see the following sections. In all cases studied, the Kantorovich method, when switched on after the second or third iteration of the standard Newton–Raphson process, converges essentially as fast as the original scheme! To avoid misunderstandings, we stress that we use the term "speed of convergence" in the meaning of the "convergence rate". In other words, it indicates how many iterations are needed to achieve a certain accuracy (or how fast the relative changes decrease with the iteration number), but not the actual computer time.

This somewhat surprising behavior may be easily understood. As already mentioned, the VEFT and other lagging techniques prevent complete linearization, in the standard variant, from converging quadratically. This deceleration of convergence caused by the lagging techniques dominates over the deceleration attributable to the fixed Jacobian, provided that the fixed Jacobian is not too different from the exact one.

The present method thus appears to be preferable over even the quasi-Newton methods, because the latter require some calculations for evaluating the updated matrix of the system, while in the former case the matrix of the system is completely known, needing only to be read from an external storage device. The computer time is then completely dominated by the formal solution step and by the I/O operations needed to read the inverted Jacobian. Both the I/O operations and the formal solution step are necessary for any method, including the quasi-Newton ones.

2.4. Acceleration by using a multi-step iteration

It is well-known from linear algebra that any iterative process

$$\boldsymbol{x}^{(n+1)}=F(\boldsymbol{x}^{(n)}) \tag{11}$$

may be significantly accelerated by using information not only from the previous iteration step, but also from still earlier steps. Such methods are now becoming widely used in the context of astrophysical radiative transfer theory, mostly for accelerating the convergence of the so-called accelerated lambda iteration (ALI) methods, for the most recent reviews; see Auer (1991) and Hubeny (1992).

The most popular of these methods is the Ng acceleration, developed by Ng (1974), and first employed in the context of ALI by Buchler & Auer (1985); a good description of the method can be found in Olson et al. (1986; hereafter OAB). Although Ng mentioned that the method may generally be used for a non-linear operator F, the method has so far been applied, in the astrophysical context, only to linear systems. Below we present one possible extension to non-linear systems.

We consider only the three-point version here. The accelerated nth iterate is taken as a linear combination of the three previous iterates

$$\boldsymbol{x}^{*}=(1-a-b)\boldsymbol{x}^{(n-1)}+a\boldsymbol{x}^{(n-2)}+b\boldsymbol{x}^{(n-3)}, \tag{12}$$

and, therefore, assuming that F in Eq. (11) is linear,

$$F(\boldsymbol{x}^{*})=(1-a-b)\boldsymbol{x}^{(n)}+a\boldsymbol{x}^{(n-1)}+b\boldsymbol{x}^{(n-2)}. \tag{13}$$

The constants a and b are then found by minimizing the quantity

$$\Omega=\sum[x_i^{*}-F(x_i^{*})]^2\,W_i, \tag{14}$$

where W is a weighting factor, taken, as recommended by OAB, as $W_i=1/x_i^{(n)}$. The detailed expressions for a and b are also presented by OAB. The iterate $\boldsymbol{x}^{(n)}$ is then replaced by the accelerated value

$$\boldsymbol{x}_{\rm acc}^{(n)}=(1-a-b)\boldsymbol{x}^{(n)}+a\boldsymbol{x}^{(n-1)}+b\boldsymbol{x}^{(n-2)}. \tag{15}$$

In the case of the Newton–Raphson process, Eq. (5), or the Kantorovich variant, Eq. (10), the operator F is given by

$$F(\boldsymbol{x})=\boldsymbol{x}-J(\boldsymbol{x})^{-1}\boldsymbol{P}(\boldsymbol{x}), \tag{16a}$$

or

$$F(\boldsymbol{x})=\boldsymbol{x}-J(\boldsymbol{X})^{-1}\boldsymbol{P}(\boldsymbol{x}), \tag{16b}$$

respectively, and is therefore non-linear. Equation (13) is not, strictly speaking, valid, but one may still use Eq. (15) for an *acceleration*. Although we do not have a rigorous mathematical proof that this procedure works for general sets of non-linear algebraic equations, nor can we state under which general conditions it works, we found empirically that it indeed works perfectly with operator F, as given by Eq. (16).

In an actual implementation of the Ng acceleration, one is essentially free to choose a particular flavor of minimization and the appropriate weighting factors. We have experimented with two different approaches. First, we minimize the residuals in all depths separately, which means letting the quantity Ω in Eq. (14), and therefore the quantities a and b, be depth-dependent. Second, we apply a global minimization, in which case Eq. (14) may be written as

$$\Omega=\sum_{d=1}^{\rm ND}\sum_{i=1}^{\rm NN}[\psi_{d,i}^{*}-F(\psi_{d,i}^{*})]^2/\psi_{d,i}^{(n)}, \tag{17}$$

assuming that $F(\psi_{d,i}^{*})$ is still (formally) given by Eq. (13). In actual computations, we proceed as follows: after a completed $I_{\rm Ng}$th iteration, where $I_{\rm Ng}$ is an input parameter (usually 6, or the iteration number where the Kantorovich variant was switched on plus 4), we perform the formal solution. Then, the constants a and b are evaluated as indicated by Eq. (17), and the accelerated vector ψ at each depth is calculated by Eq. (15). We then perform another formal solution step, and, finally, perform the next linearization iteration, i.e. the steps (i)–(iii) of solving Eqs. (8) and (9) (with matrices A_d, B_d, C_d, D_d either being recalculated – in the ordinary variant, or with the appropriate matrices D_d, $(B_d-A_dD_{d-1})^{-1}$, and A_d being read from the external storage device – in the Kantorovich variant); see Fig. 1. The second formal solution step performed after the acceleration is very important, otherwise one would enter the next iteration of complete linearization with an inconsistent radiation field and level populations, which would significantly slow down the convergence process or may even lead to divergences.

As expected, the global minimization, Eq. (17), exhibits much better convergence properties in most cases studied. Therefore, we adopt Eq. (17) in all the following calculations. Other free parameters are the iteration number where the accelerated vector is calculated for the first time, $I_{\rm Ng}$, and the number of iterations between successive accelerations, $\Delta I_{\rm Ng}$. The acceleration cannot be started earlier than in the fourth iteration, but this value is seldom of any practical use, since the first few iterations always exhibit large relative changes. We have found that the acceleration process may be safely started between the fifth and the seventh iteration, and may be repeated each fifth iterations. We have experimented with other values of $\Delta I_{\rm Ng}$, such as 1 or 2, but these values generally slowed down the iteration process.

As another practical matter, we did not want to mix iterates originating in the ordinary Newton–Raphson cycles with those calculated in the Kantorovich iterations. Therefore, if Ng acceleration was used together with the Kantorovich variant, we started the Ng acceleration four iterations after the Kantorovich variant was switched on. In such cases we could probably have started the Ng acceleration earlier, leading to further savings of computer time, but since the time needed to perform one or two more Kantorovich iterations would not have been an appreciable portion of the total time, this was not done.

As we shall show in the next section, the Ng acceleration introduces an essential improvement in convergence for both the standard and the Kantorovich versions. However, it is the synergistic *combination* of the Kantorovich version and the Ng acceleration which offers a very attractive method for calculating model stellar atmospheres.

3. Test cases

In order to test the proposed methods for a wide range of stellar atmospheric parameters and still keep the number of test cases reasonably small, we have chosen to calculate models for three different effective temperatures, $T_{\rm eff}=10\,000$, 25 000, and 50 000 K. In all cases, $\log g=4$, and solar composition was adopted. These roughly correspond to main-sequence early A, B, and O stars, respectively. The range of effective temperature covers nearly the entire range of models where the complete linearization has been applied. For cooler stars, the NLTE effects are believed to play a minor role in their photospheres; the main concern here is a proper treatment of the (LTE) line blanketing.

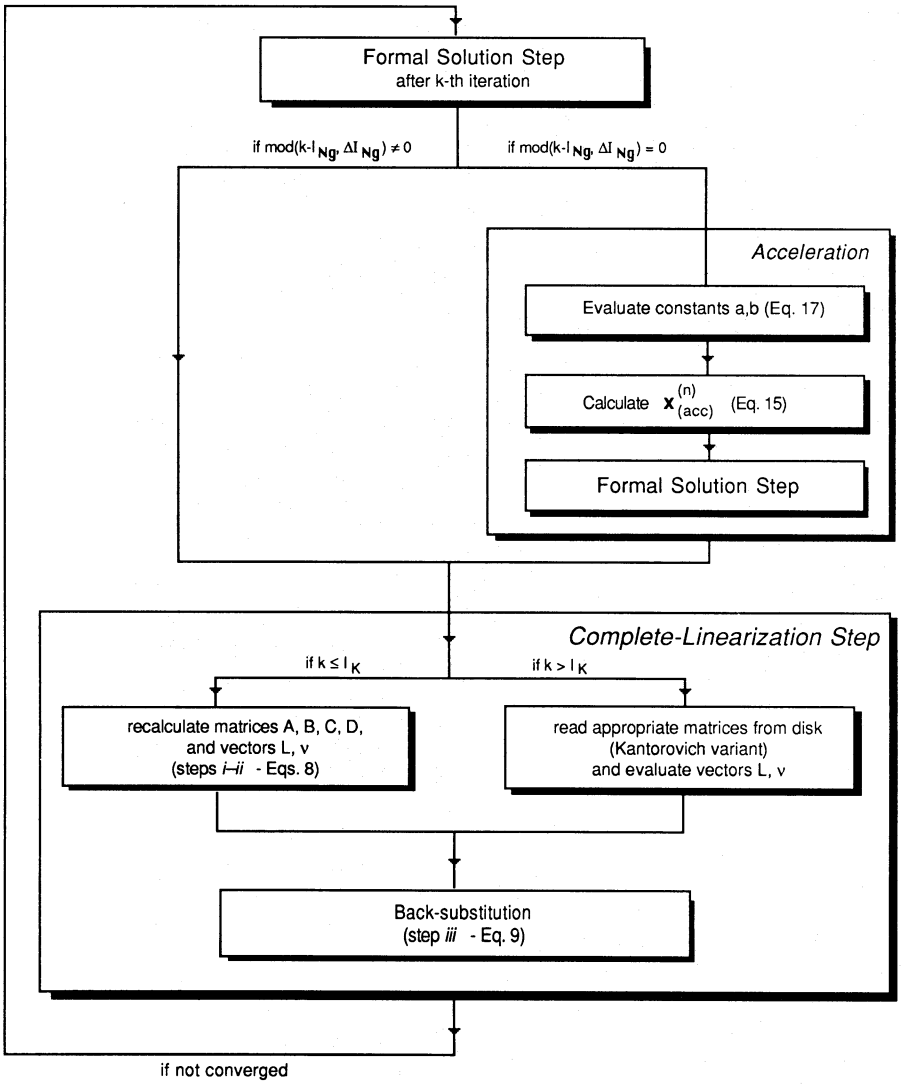

Fig. 1. A flow-chart diagram of one iteration of the complete-linearization method, improved by the two acceleration schemes discussed in the present paper, the Kantorovich variant, and the Ng acceleration. k denotes the current iteration, I_K is the iteration where the Kantorovich variant was switched on, I_{Ng} is the iteration where the Ng acceleration was performed for the first time, and ΔI_{Ng} is the number of iterations between two accelerations

Models hotter than 50 000 K are usually rather easy to calculate (that is, within the frame of the "classical" model defined above), and the convergence behavior of the 50 000 K model may be viewed as representative for hotter models as well.

For every effective temperature, the final model was calculated in the usual sequence LTE-grey model→LTE model→NLTE/C model (NLTE with continua only)→NLTE/L model (NLTE including lines). Table 1 summarizes the basic properties of the models. The models were calculated for the purposes of testing their convergence properties only. We avoided very simplistic models, because their convergence properties would not necessarily be indicative of the behavior of the more complex models likely to be used in actual research. On the other hand, we also avoided very sophisticated models, because they would have required excessive computer time, worth spending for purposes of actual spectroscopic diagnostics, but not for our purposes here. Since we intended to explore the convergence properties of many different algorithms in detail, we let each model converge to a much higher accuracy (the maximum relative change of all quantities at all depths less than 10^{-5}) than needed for any practical purpose.

Table 1. General characteristics of the model stellar atmospheres: Number of NLTE levels, depth points, lines (total and linearized) and frequencies (total and linearized)

Model	NLTE Levels				ND	Lines		Frequencies	
	H	He I	He II	other		tot.	(lin.)	tot.	(lin.)
T10LT	9	–	–	–	94	–	–	63	(63)
T10NC	9	–	–	–	94	–	–	63	(63)
W10NC	9	–	–	–	94	–	–	1089[a]	(112)
T10NL	9	–	–	–	94	21	(6)	255	(138)
W10NL	9	–	–	–	94	21	(6)	1232[a]	(138)
T25NC	13	14	1	–	70	–	–	55	(55)
T25NL	13	14	1	–	70	74	(18)	403	(161)
T50NC	13	14	14	16	70	–	–	72	(72)
T50NL	13	14	14	16	70	159	(12)	711	(123)

[a] Includes 1007 internal frequency points for NLTE ODFs.

3.1. 50 000 K model

The hottest models assume an atomic level structure similar to models already used before (Hubeny et al. 1991). Departures from LTE are allowed for first 12 levels of H, 14 levels of He II, 14

levels of He I (all LS states for $n=2$ treated as separate levels, and higher states up to $n=8$ appropriately averaged; singlet and triplet states up to $n=5$ are treated separately). Moreover, we include a few low-lying states of C III–C V, N III–N V, O IV–O VI (altogether 16 levels). In addition, we include the effects of wind blanketing, with an albedo equal to 0.04 in all continua except the He II Lyman continuum, where the albedo is set to 0.8, and in hydrogen and helium lines where the albedo used is 0.1 (representative of typical values for an early O star). The effects of a microturbulent velocity, $v_{tb}=25$ km s^{-1}, are included in the line broadening as well as in the total pressure (see also Hubeny et al. 1991). All allowed hydrogen and helium lines are considered, except the He II Lyman lines, for which detailed radiative balance is assumed. For lines, we assume depth-independent Doppler profiles.

3.2. *25 000 K model*

The intermediate-temperature model ($T_{\rm eff}=25\,000$ K) considers only hydrogen and neutral helium (the ionized helium is represented by a one-level ion). Again, we take 12 and 14 NLTE levels for H and He I, respectively, and consider all transitions between them, except the resonance lines of He I, which are assumed to be in detailed radiative balance.

3.3. *10 000 K model*

Construction of a NLTE model atmosphere for $T_{\rm eff}=10\,000$ K, even for the simplest pure-hydrogen composition, presents a nontrivial problem, as the previous history of various attempts attests (Kudritzki 1973; Frandsen 1974; Borsenberger & Gros 1978; Hubeny 1981, 1986). We consider two different types of models. First, an almost "classical" model (similar to the previous studies, only slightly extended) – 8 NLTE levels of H I plus one level of H II, 21 lines between them (all except Lyman lines which are assumed to be in detailed radiative balance), and Doppler profiles for all lines. Second, we also consider much more sophisticated, albeit still pure-hydrogen, models, considering detailed, Stark + Doppler profiles for all Balmer and higher Lyman lines (low members of the Lyman series are still considered with detailed radiative balance) and allowing for the effects of a detailed opacity due to high members of the Lyman and Balmer series. The latter opacity, treated within the framework of the generalized occupation probability formalism (Hummer & Mihalas 1988), is essentially exact. Also, a dissolution of Rydberg states is treated essentially exactly. The opacity near the Lyman and Balmer series limits, which is represented by a total of 1007 internal frequency points, is described through a newly introduced *NLTE opacity distribution functions* (ODF), which enables us to represent this opacity by means of only 30 frequency points in the linearization step. This algorithm takes into account the effects of higher lines both in radiative equilibrium (via opacities) and in statistical equilibrium (via modified radiative rates into and out of levels $n=1$ and $n=2$). Note that the usual mark of quality of a model, the number of lines which are taken into account, here loses its well-defined meaning, since in this formalism the number of lines depends on depth, via the dissolution of Rydberg states. A detailed description will be presented in a forthcoming paper (Hubeny et al. 1992).

3.4. *Computational considerations*

All calculations reported below were made with the appropriately modified computer program TLUSTY (Hubeny 1988). A new version, which incorporates the new acceleration algorithms, the NLTE opacity distribution option, and which also is now better vectorized for the use on Cray computers, is available from the authors upon request. It is also distributed via the Collaborative Computer Project No. 7 (CCP7-"Analysis of Astronomical Spectra") computer programs library. The new version of TLUSTY was also thoroughly optimized, so that it now requires, even in the standard variant without any acceleration discussed in the present paper, about 60–75% of the time needed to run the same model with the older code (i.e. versions up to serial number TLUSTY154). On Cray computers, the new version now works up to six times faster.

Although we have run the program on various computers (VAX, Cray YMP), we have decided to calculate the whole set of models, for the purposes of the present paper, on a DEC 5000/200 workstation (with 25 MHz clock speed, 24 MIPS, 3.7 MFLOPS, 18.5 SPECmark). We believe that the timing comparisons based on runs on the workstation are more indicative, since workstations are becoming more and more widely available.

4. Results and discussion

Figures 2 and 3 show the convergence properties and the effects of acceleration algorithms for two models in detail. Figure 2 shows a typical case of "fast convergence" behavior, for the NLTE/C model with $T_{\rm eff}=10\,000$ K (T10NC). The left side shows iterations of the ordinary, non-accelerated, complete linearization, while the right side displays the convergence history for the model where the Kantorovich variant was switched on after the second iteration and the Ng acceleration was performed after the seventh iteration. The upper panels display the logarithm of the relative changes in temperature, and the lower panels display the logarithm of the maximum relative change of all quantities, both as a function of depth.

This figure illustrates three important features. First, the convergence of complete linearization, even in the standard variant, is global and rather fast – about 0.4 dex per iteration. In this case there are no fixed radiative rates, and the only "lagged" quantities are the Eddington factors. Second, the relative changes for the third to sixth iterations are virtually the same in both cases, which demonstrates that *the Kantorovich variant does not slow down* the convergence rate with respect to the standard case. And, third, the effect of Ng acceleration is rather dramatic. The total number of iterations to achieve $\max|\delta\psi_{i,d}/\psi_{i,d}|<10^{-5}$ everywhere dropped from 14 to 8!

Figure 3 displays, in contrast, the most difficult case, an example of the slowest convergence, model W10NL. From the total of 1232 frequency points considered in model construction, the radiation intensity is linearized in only 138 points. In a straightforward application of complete linearization, the matrices of the system would be about 10 times larger, which would increase the computer time by the factor of 1000! In our algorithm, the lagging slows down the convergence considerably: the rate of convergence is now about 0.125 dex per iteration, about three times slower than in the previous, fast-convergent, model, but the convergence is still *uniform* and *global*. (Needless

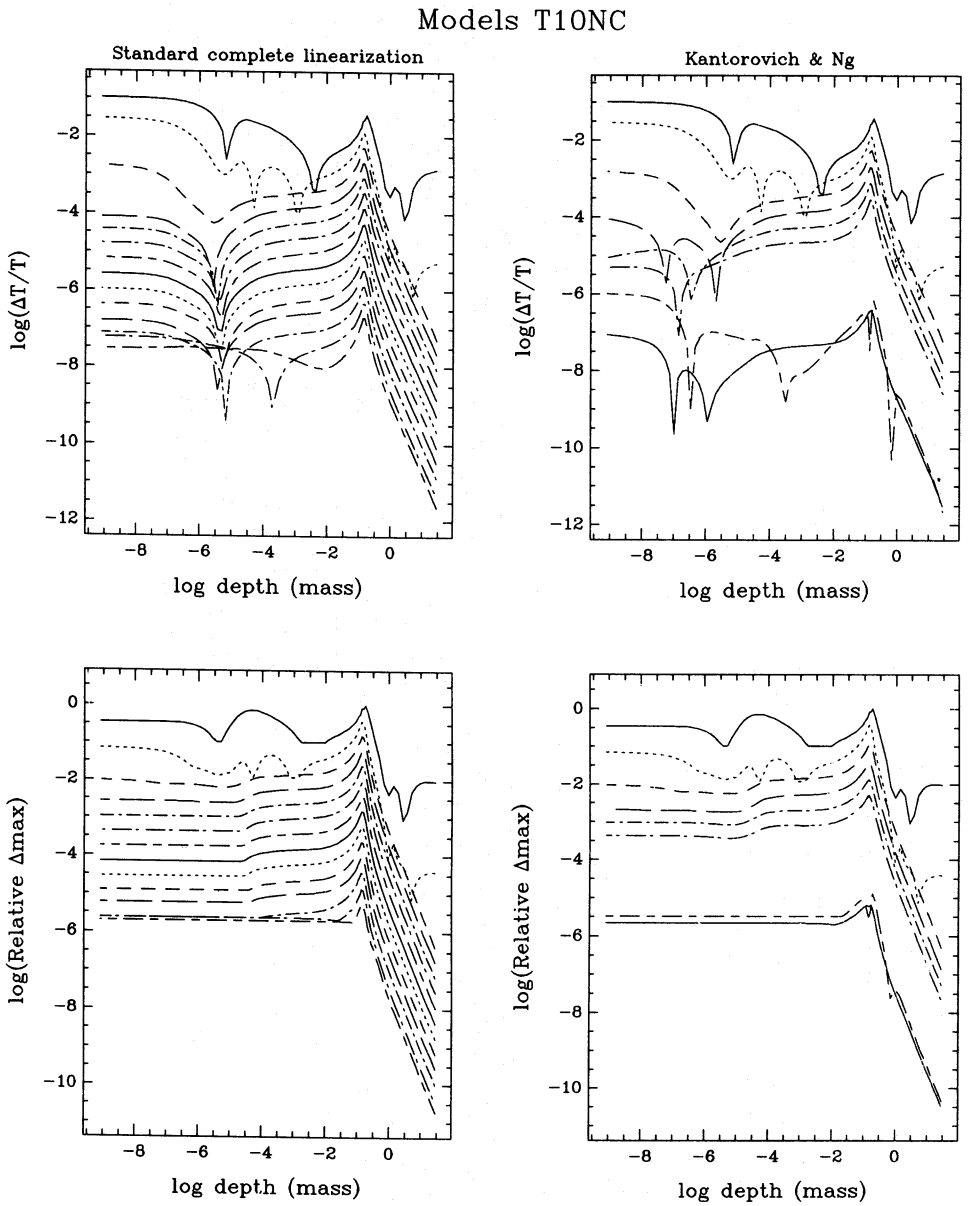

Fig. 2. Detailed convergence behavior of the model T10NC (i.e. the NLTE/C model with $T_{\rm eff} = 10\,000$ K). The left hand panels: standard complete linearization; the right hand panels: models calculated by the Kantorovich variant (switched on after the second iteration), together with the Ng acceleration (performed in the seventh iteration). The upper graphs display $\log|\delta T/T|$ as a function of depth (taken as a column mass in g cm^{-2}); the lower graphs display the maximum relative changes of all elements of the state vector, ψ, as a function of depth. The line pattern is repeated every 8th iteration; the upper full line corresponds to the first iteration, the dotted line to the second iteration, etc. Notice the global, almost monotonic convergence. The effect of Ng acceleration is best seen in the lower right panel

to say, the net time-gain with respect to a straightforward linearization amounts to a factor of 300 or more, which more than validates the usefulness of lagging).

The right panel shows the convergence in the case of Kantorovich variant, accelerated by the Ng algorithm. Again, the effect is dramatic. Most importantly, the relative time-gain using acceleration is much more pronounced in the complicated models than in simple models, as for instance the one displayed in Fig. 2. This is precisely the feature which makes the present acceleration methods very attractive, since more realistic, and therefore more complicated, models are badly needed to match the high quality of the present-day spectrophotometric observations. This example also demonstrates that the Ng acceleration nicely complements the idea of reducing the size of matrices by employing the lagging techniques: a decreased rate of convergence due to lagging is compensated by the use of Ng acceleration. But, in addition, the time per iteration using the Kantorovich variant is now substantially diminished, so that the final time-gain may be enormous.

The next set of figures (Figs. 4–7) displays the convergence and timing properties of various acceleration schemes in a synoptic form. In each figure, the lower panel shows the maximum relative change in temperature as a function of the iteration number, while the upper panel shows the time consumption on a DECstation 5000/200. The filled circles at the ends of lines indicate the total time needed to obtain the final, very accurate model ($\max|\delta\psi_{i,d}/\psi_{i,d}| < 10^{-5}$) in the absence of Ng acceleration, while the triangles indicate the time to achieve the same accuracy using the Ng acceleration. The lines representing time consumption for the Ng acceleration cases are almost indistinguishable from their unaccelerated counterparts, which reflects the fact that the extra time needed to set up the acceleration parameters – Eqs. (15) and (17) – is negligible.

Figure 4 displays the LTE and NLTE/C models for $T_{\rm eff} = 10\,000$ K. Again, the effects of Ng acceleration are clearly seen. Also, we see that the Kantorovich variant, when switched on already at the first iteration, converges slower than the ordinary complete linearization (however, the total computer time is

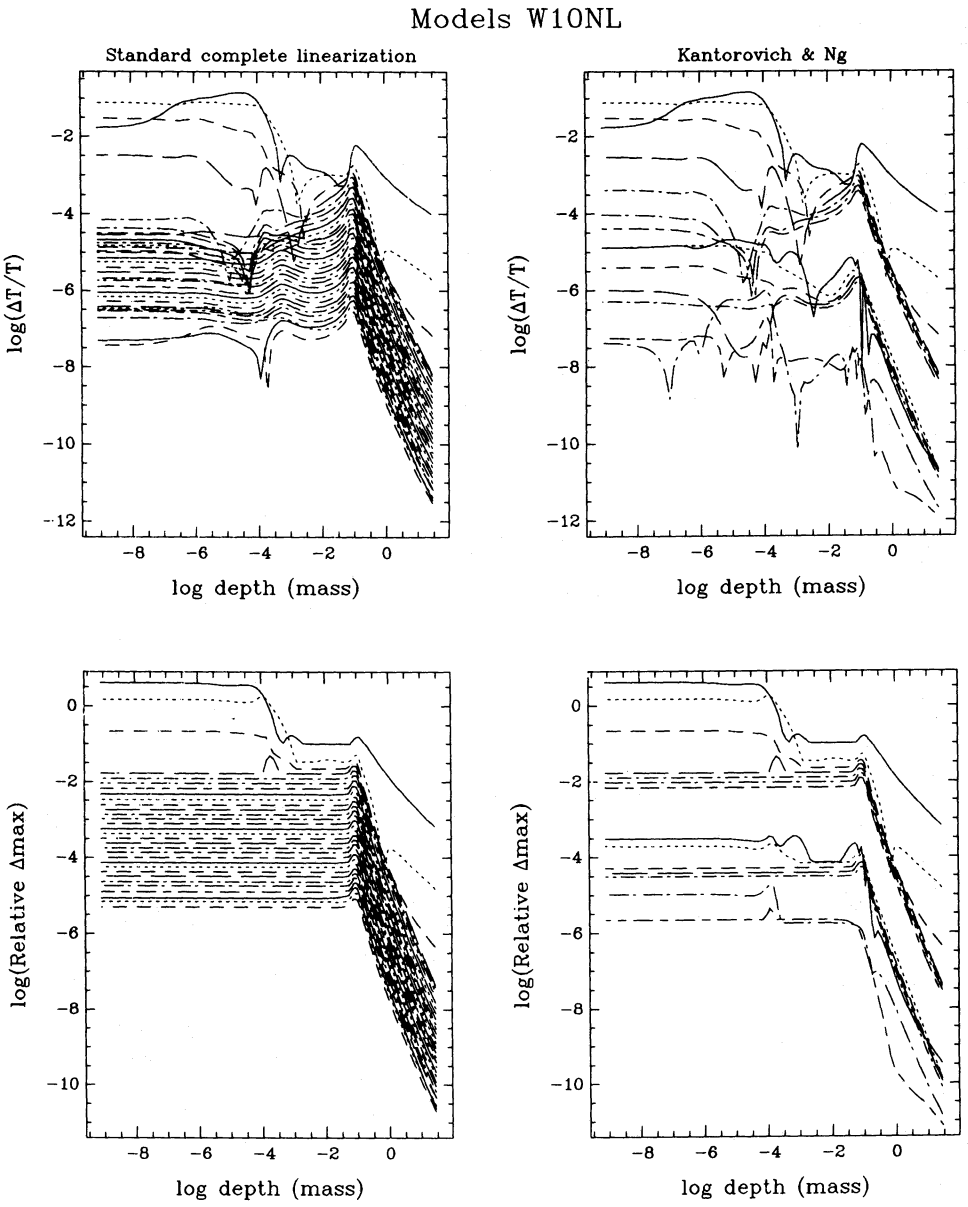

Fig. 3. The same as in Fig. 2, but for the model W10NL. Notice a much slower (but still global, stable, and monotonic), convergence of the standard variant than that displayed in Fig. 2, and the dramatic effect of the Ng acceleration (performed after the seventh and twelfth iteration; the Kantorovich variant was switched on after the third iteration)

still much shorter than in the standard case), while if switched on after the second iteration it converges as fast as the standard variant.

In the case of LTE and NLTE/C models, the slopes of lines representing the computer time as a function of iteration number (upper panel) for ordinary complete linearization and the Kantorovich variant are not as different as one might expect. This reflects the fact that the formal solution step and the I/O operations consume an appreciable portion of the total time.

Figure 5 again shows the very favorable properties of the Kantorovich variant and the Ng acceleration for the involved model (W10NL). The convergence behavior is quite analogous for hotter models as well, as displayed in Fig. 6 (for NLTE/L model with $T_{\rm eff}=25\,000$ K), and Fig. 7 (NLTE/L model with $T_{\rm eff}=50\,000$ K). As pointed out above, one should be cautious about switching on the Kantorovich variant too soon. NLTE models with lines are, so to speak, "more non-linear" than NLTE/C or LTE models, and consequently keeping the Jacobian fixed as soon as the first or second iteration may significantly slow down the convergence, or even lead to divergences (see Figs. 5 and 7). The safe, and therefore recommended, strategy is to fix the Jacobian only after the third iteration. Figure 5 also shows a very interesting feature: the Ng acceleration is even able to turn an otherwise divergent iteration process into convergence, as was the case when the Kantorovich variant was switched on after the second iteration.

The models discussed in the figures were converged to a very high accuracy, which is usually not required for practical purposes. Therefore, we present, in Tables 2–4, time comparisons for three different convergence criteria: (i) $\max|\delta T_d/T_d|<10^{-3}$ (acceptable only for exploratory model calculations), (ii) $\max|\delta\psi_{i,d}/\psi_{i,d}|<10^{-3}$ (the recommended criterion), and (iii) $\max|\delta\psi_{i,d}/\psi_{i,d}|<10^{-5}$, our "high-accuracy" criterion. For the least stringent criterion, the time-gain using the Kantorovich

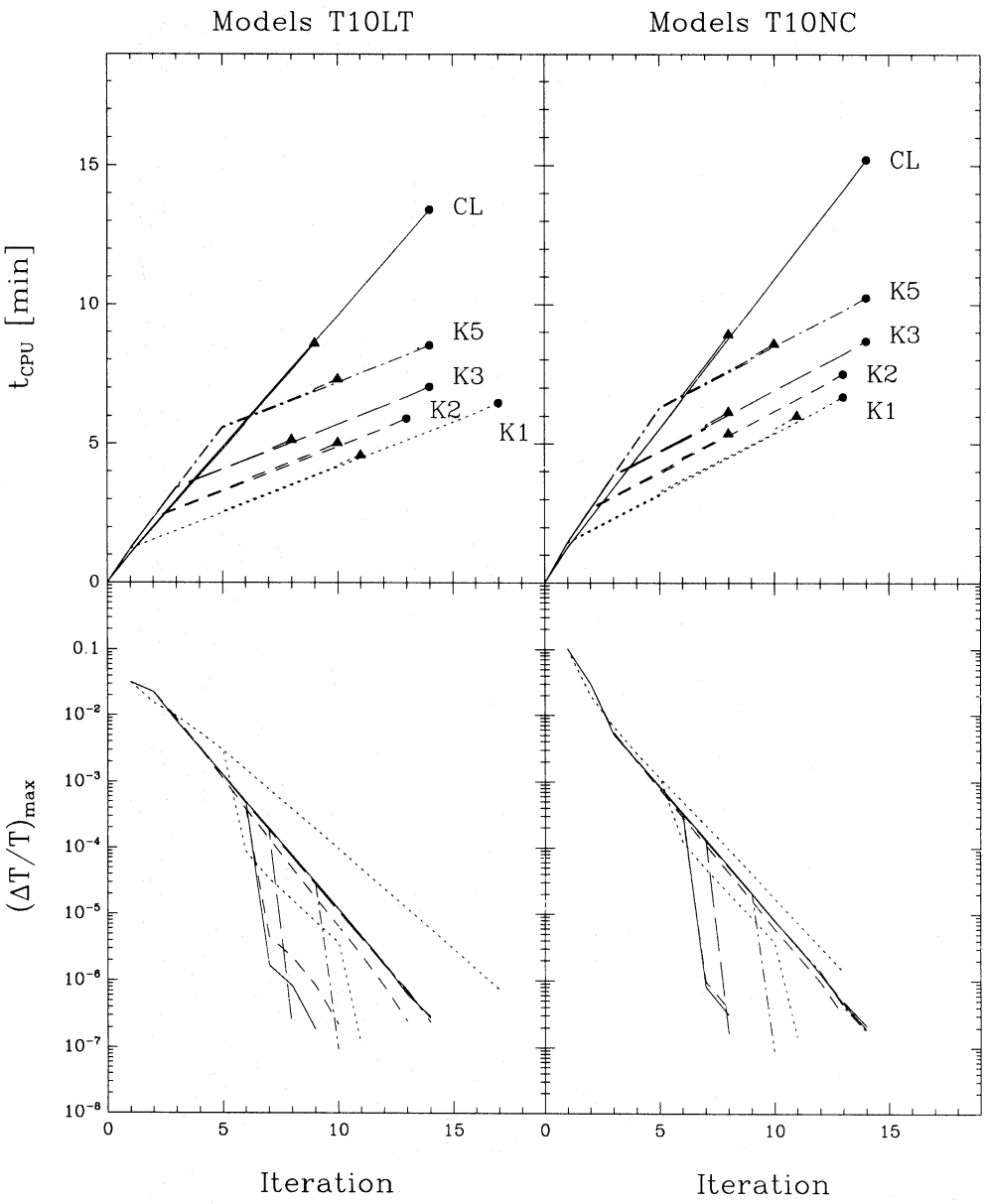

Fig. 4. Convergence and timing properties of the models T10LT (the left panel), and T10NC (the right panel). The upper panel shows the computer time on a DECstation 5000/200 as a function of the iteration number for various acceleration parameters. The filled circles at the endpoints of lines indicate the total time needed to obtain the final model with high accuracy ($\max|\delta\psi_{i,d}/\psi_{i,d}|<10^{-5}$); the triangles indicate the time needed to obtain the model of the same accuracy using the Ng acceleration. The full lines, labeled CL, represent the standard complete linearization; the other lines, labeled Kn, represent the Kantorovich variant, where the Jacobian was held fixed after the nth iteration. The lower panel displays the maximum $|\delta T/T|$ over all depths as a function of the iteration number. The various lines represent the same models as in the upper panel. The unaccelerated models exhibit a more or less monotonic decrease of maximum relative change with the iteration number, while the models with Ng acceleration show a sudden, conspicuous decrease of the relative change immediately after the acceleration

variant is the smallest; actually, for very simple and fast-convergent models (LTE or NLTE/C models), the Kantorovich variant may even not be useful at all if switched on too late (e.g., when switched on after fifth iteration for model T10NC; see Table 2). However, for the moderately stringent criterion (the middle section of Tables 2–4), the Kantorovich variant leads to a time gain in all models. We stress again that the absolute time gain tends to be more pronounced for more complex models.

5. Conclusions

We have discussed two means of accelerating the ordinary complete-linearization method. The first is the Kantorovich variant, which consists of keeping the Jacobi matrix of the system fixed. The most time-consuming part of the calculations – the inversion of the Jacobian – is therefore avoided, and the computation time is dominated by the formal solution step and by the I/O operations needed to store and read the fixed inverted Jacobian. In machines with a very large internal memory, or for relatively simple problems, one may keep the whole inverted Jacobian in memory (we need to store matrices D_d, $(B_d - A_d D_{d-1})^{-1}$, and A_d for all depths, which requires of the order of $2 \times \mathrm{ND} \times \mathrm{NN}^2$ words); this would lead to a further reduction of the computer time. Application of the Kantorovich variant involves a free, adjustable parameter, namely the iteration number after which it is switched on. As a rule of thumb, we found that keeping the Jacobian fixed after the second iteration for LTE and NLTE/C models, and after the third iteration for NLTE/L models, represents the safest option, applicable to all models calculated so far. Originally, we tested another criterion for switching on the Kantorovich variant, namely the iteration where the maximum relative change of all quantities at all depths drops below some previously selected value (e.g. 5, 20, or 50% etc.). We later found

Table 2. Convergence properties of models with $T_{\rm eff} = 10\,000$ K

Kantor.	Ng		max $\lvert\delta T/T\rvert < 10^{-3}$			max $\lvert\delta\psi_{\rm d,i}/\psi_{\rm d,i}\rvert < 10^{-3}$			max $\lvert\delta\psi_{\rm d,i}/\psi_{\rm d,i}\rvert < 10^{-5}$		
start	start	step	IT	$t_{\rm CPU}$ [s]	ratio	IT	$t_{\rm CPU}$ [s]	ratio	IT	$t_{\rm CPU}$ [s]	ratio
Models **T10LT**											
–	–	–	6	350.7	1.00	9	520.5	1.00	14	806.9	1.00
–	6	5	6	347.2	0.99	7	403.4	0.78	9	517.7	0.64
5	–	–	6	355.4	1.01	9	414.1	0.80	14	513.8	0.64
5	9	5	6	357.8	1.02	9	419.0	0.81	10	440.7	0.55
3	–	–	6	265.3	0.76	9	324.3	0.62	14	424.7	0.53
3	7	5	6	266.7	0.76	8	310.5	0.60	8	310.5	0.38
2	–	–	6	218.1	0.62	8	257.2	0.49	13	356.9	0.44
2	6	5	6	223.4	0.64	7	243.1	0.47	10	303.9	0.38
1	–	–	7	192.5	0.55	11	270.9	0.52	17	390.2	0.48
1	5	5	6	175.6	0.50	7	195.1	0.37	11	277.9	0.34
Models **T10NC**											
–	–	–	5	335.9	1.00	9	592.5	1.00	14	915.8	1.00
–	6	5	5	334.6	1.00	7	471.3	0.80	8	537.9	0.59
5	–	–	5	382.0	1.14	9	485.8	0.82	14	618.1	0.67
5	9	5	5	379.0	1.13	9	489.4	0.83	10	517.3	0.56
3	–	–	5	287.7	0.86	9	391.4	0.66	14	523.6	0.57
3	7	5	5	284.3	0.85	8	371.8	0.63	8	371.8	0.41
2	–	–	5	242.5	0.72	8	320.6	0.54	13	453.0	0.49
2	6	5	5	238.2	0.71	7	297.6	0.50	8	325.5	0.36
1	–	–	6	220.7	0.66	8	272.7	0.46	13	404.6	0.44
1	5	5	6	224.8	0.67	6	224.8	0.38	11	362.7	0.40
Models **W10NC**											
–	–	–	4	1292.3	1.00	7	2144.6	1.00	11	3286.7	1.00
–	6	5	4	1277.2	0.99	7	2143.0	1.00	7	2143.0	0.65
5	–	–	4	1398.9	1.08	7	1843.4	0.86	11	2120.2	0.65
5	9	5	4	1388.8	1.07	7	1830.1	0.85	10	2057.0	0.63
3	–	–	4	1156.7	0.90	7	1361.2	0.63	11	1639.8	0.50
3	7	5	4	1144.7	0.89	7	1365.5	0.64	8	1438.5	0.44
2	–	–	4	915.7	0.71	7	1120.2	0.52	11	1398.6	0.43
2	6	5	4	910.0	0.70	7	1136.5	0.53	7	1136.5	0.35
1	–	–	7	909.2	0.70	10	1112.1	0.52	18	1659.2	0.50
1	5	5	6	864.7	0.67	8	998.7	0.47	15	1493.2	0.45
Models **T10NL**											
–	–	–	6	3250.9	1.00	13	6971.4	1.00	23	12259.8	1.00
–	6	5	6	3204.2	0.99	8	4255.7	0.61	14	7403.5	0.60
5	–	–	6	3015.7	0.93	13	3652.2	0.52	23	4533.4	0.37
5	9	5	6	2947.0	0.91	11	3403.0	0.49	15	3758.0	0.31
3	–	–	7	2151.8	0.66	14	2780.0	0.40	24	3662.3	0.30
3	7	5	7	2100.7	0.65	9	2278.4	0.33	13	2632.5	0.21
2	–	–	8	1771.8	0.55	14	2306.9	0.33	25	3277.3	0.27
2	6	5	10	1887.6	0.58	13	2154.2	0.31	18	2591.4	0.21
Models **W10NL**											
–	–	–	5	2895.2	1.00	15	8202.7	1.00	31	16666.3	1.00
–	6	5	5	2912.3	1.01	7	4011.5	0.49	13	7237.3	0.43
5	–	–	5	3110.1	1.07	16	4109.4	0.50	32	5536.8	0.33
5	9	5	5	3103.6	1.07	10	3595.2	0.44	14	3955.7	0.24
3	–	–	5	2133.8	0.74	16	3133.3	0.38	32	4559.9	0.27
3	7	5	5	2167.7	0.75	8	2476.5	0.30	14	3042.0	0.18

that this criterion was not very useful, since the procedure worked well even if the maximum change is still around 100%.

The second method is an application of the Ng acceleration. It may be used either in conjunction with the standard complete linearization, or with the Kantorovich variant. In both cases, the Ng acceleration indeed leads to a substantial reduction of the computer time, but the time-gain is most significant if it is used along with the Kantorovich variant. Again, the adjustable parameters are the iteration number where the acceleration is first performed, and the number of iterations between two accelerations. We have tested several possibilities, and found that the best results are obtained with the first parameter equal to 6 (in the case of standard Newton–Raphson linearization), or the starting Kantorovich iteration plus 4; and with 5 normal iterations between successive accelerations. These values may not necessarily represent the optimum choice in all cases; however, we believe that they are reasonable for most users.

These acceleration schemes also very nicely complement the idea of fixed rates, or of general lagging techniques, employed systematically in the previous versions of TLUSTY (Hubeny

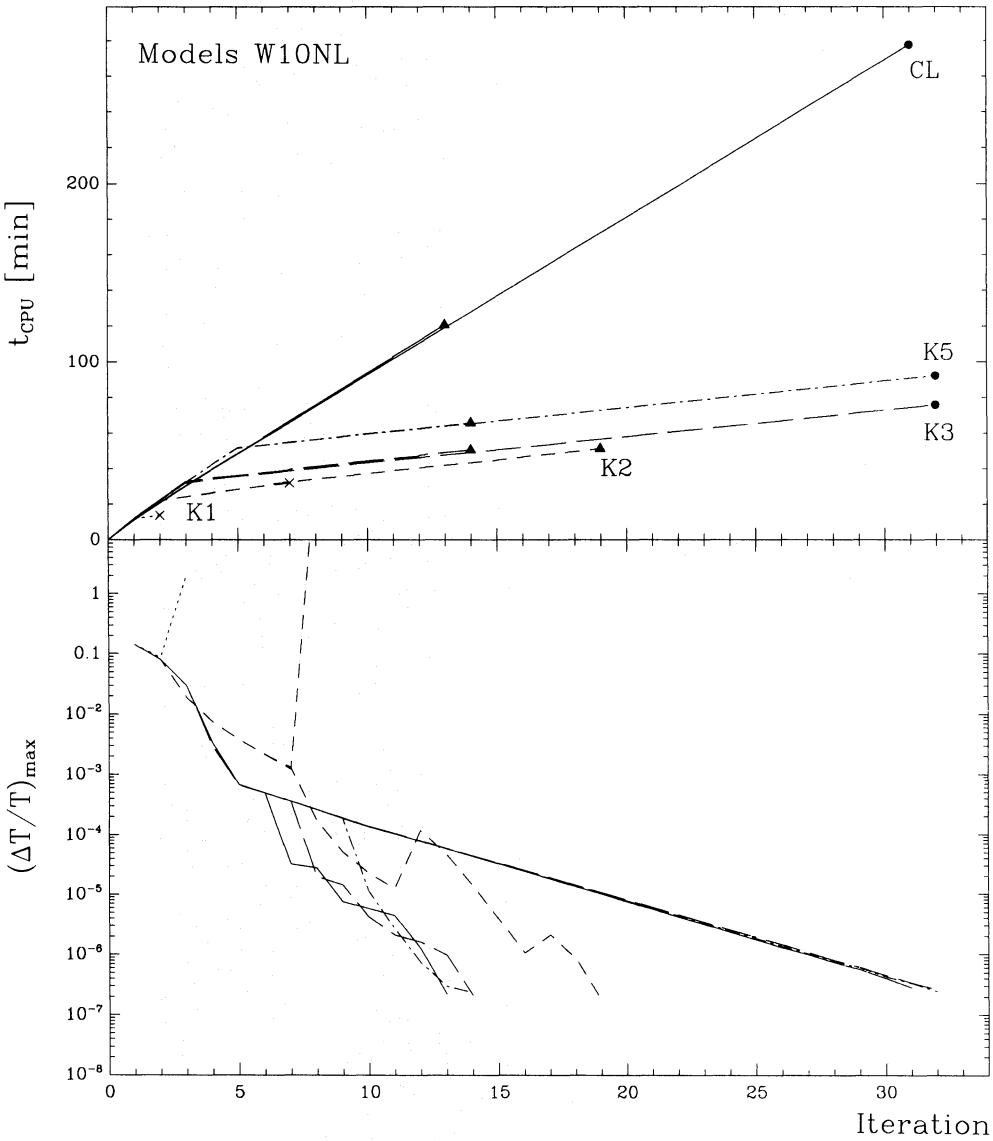

Fig. 5. The same as in Fig. 4, but for models W10NL. Notice the divergence in the case when the Jacobian is held fixed too early. The crosses in the upper panel indicate the iteration where the corresponding model has diverged

Table 3. Convergence properties of models with $T_{eff} = 25\,000$ K

Kantor.	Ng		max $\lvert\delta T/T\rvert < 10^{-3}$			max $\lvert\delta\psi_{d,i}/\psi_{d,i}\rvert < 10^{-3}$			max $\lvert\delta\psi_{d,i}/\psi_{d,i}\rvert < 10^{-5}$		
start	start	step	IT	t_{CPU} [s]	ratio	IT	t_{CPU} [s]	ratio	IT	t_{CPU} [s]	ratio
Models **T25NC**											
–	–	–	4	332.8	1.00	4	332.8	1.00	5	413.5	1.00
–	6	5	4	328.2	0.99	4	328.2	0.99	5	408.1	0.99
3	–	–	4	308.3	0.93	4	308.3	0.93	5	343.5	0.83
3	7	5	4	312.6	0.94	4	312.6	0.94	5	347.5	0.84
2	–	–	4	257.5	0.77	5	289.7	0.87	8	389.4	0.94
2	6	5	4	259.0	0.78	5	291.1	0.87	7	374.3	0.91
1	–	–	7	302.3	0.91	11	430.3	1.29	19	688.3	1.66
1	5	5	6	286.4	0.86	9	383.3	1.15	12	499.0	1.21
Models **T25NL**											
–	–	–	5	4592.8	1.00	7	6403.4	1.00	12	10815.7	1.00
–	6	5	5	4424.0	0.96	7	6211.5	0.97	11	9702.4	0.90
5	–	–	5	4651.0	1.01	7	4888.1	0.76	12	5458.7	0.50
5	9	5	5	4674.0	1.02	7	4912.2	0.77	12	5522.1	0.51
3	–	–	5	3040.7	0.66	7	3276.4	0.51	12	3844.0	0.36
3	7	5	5	3037.5	0.66	7	3308.5	0.52	11	3765.8	0.35
2	–	5	7	2475.9	0.54	10	2820.5	0.44	13	3152.2	0.29
2	6	5	7	2515.8	0.55	7	2515.8	0.39	12	3111.2	0.29
1	–	–	11	2132.5	0.46	15	2569.4	0.40	23	3446.5	0.32
1	5	5	7	1715.8	0.37	11	2197.1	0.34	17	2884.1	0.27

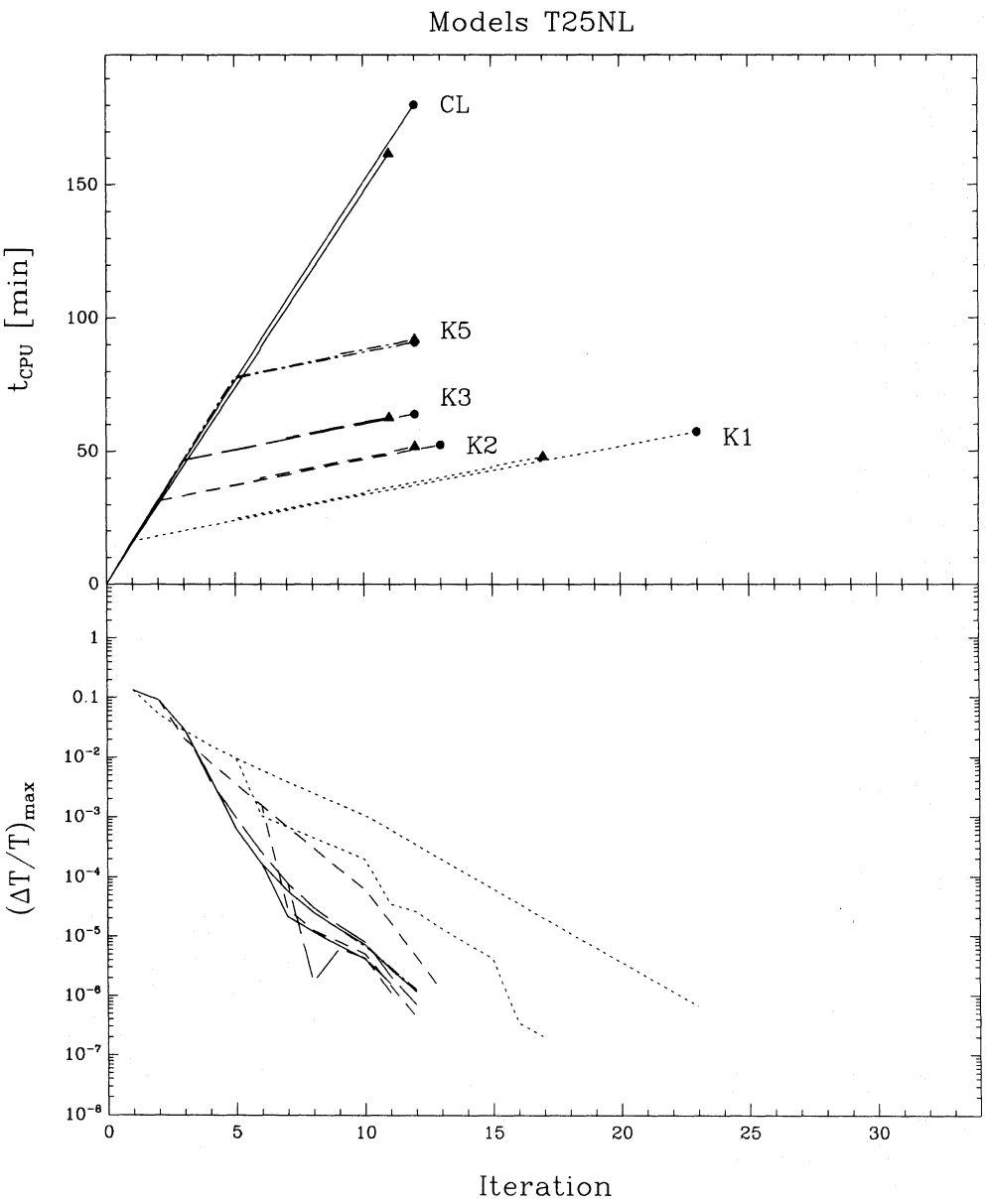

Fig. 6. The same as in Fig. 4, but for models T25NL

Table 4. Convergence properties of models with $T_{eff} = 50\,000$ K

Kantor. start	Ng start	Ng step	max $\lvert\delta T/T\rvert < 10^{-3}$ IT	t_{CPU} [s]	ratio	max $\lvert\delta\psi_{d,i}/\psi_{d,i}\rvert < 10^{-3}$ IT	t_{CPU} [s]	ratio	max $\lvert\delta\psi_{d,i}/\psi_{d,i}\rvert < 10^{-5}$ IT	t_{CPU} [s]	ratio
Models **T50NC**											
–	–	–	5	1510.2	1.00	5	1510.2	1.00	7	2089.6	1.00
–	6	5	5	1501.6	0.99	5	1501.6	0.99	7	2133.7	1.02
5	–	–	5	1625.0	1.08	5	1625.0	1.08	7	1811.2	0.87
5	9	5	5	1579.1	1.05	5	1579.1	1.05	7	1762.5	0.84
3	–	–	5	1159.6	0.77	6	1248.1	0.83	9	1518.7	0.73
3	7	5	5	1157.7	0.77	6	1246.0	0.83	8	1479.9	0.71
2	–	–	4	869.8	0.58	17	2025.7	1.34	33	3455.3	1.65
2	6	5	4	848.7	0.56	12	1654.3	1.10	14	1836.7	0.88
Models **T50NL**											
–	–	–	8	6382.6	1.00	14	11019.7	1.00	21	16421.0	1.00
–	6	5	7	5666.4	0.89	12	9604.9	0.87	17	13523.2	0.82
5	–	–	8	4655.3	0.73	13	5325.1	0.48	20	6251.0	0.38
5	9	5	8	4685.5	0.73	13	5433.0	0.49	15	5762.6	0.35
3	–	–	8	3322.5	0.52	13	3994.2	0.36	19	4787.1	0.29
3	7	5	8	3397.8	0.53	12	3993.9	0.36	15	4394.1	0.27

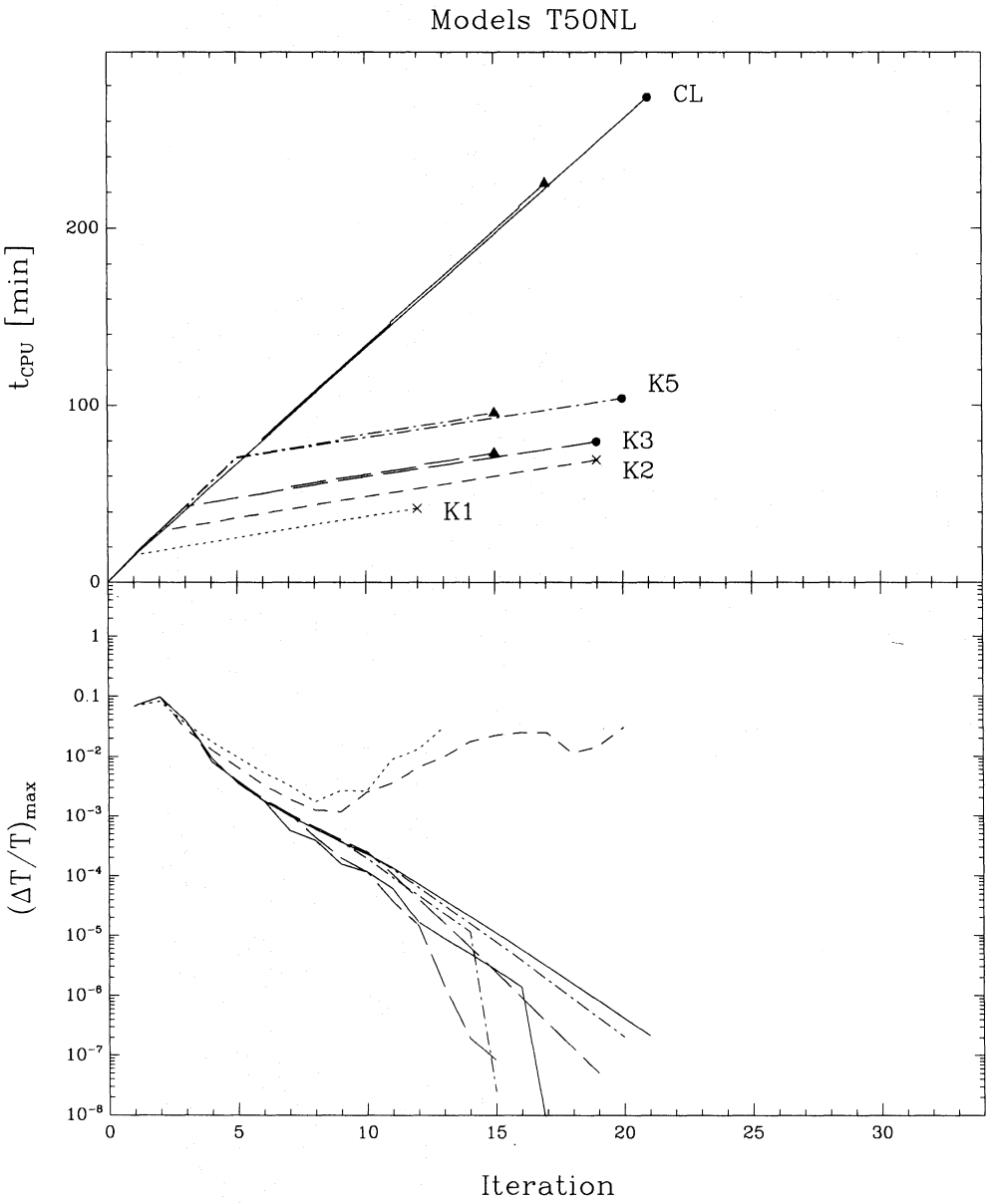

Fig. 7. The same as in Fig. 5, but for models T50NL

1988). With extensive use of lagged quantities, previous versions of the code would eventually converge, but at much slower rates. (Indeed, if there were too many fixed transitions, or if one uses the fixed rate option for strong resonance lines, the lagging behaves similarly as the ordinary Lambda iteration). However, even with the Kantorovich variant alone, the lagging, even if extensive, becomes useful again since the Kantorovich variant reduces the time per iteration significantly, while keeping the convergence rate unchanged. One may therefore easily afford many iterations, say 30 or even more. Applying the Ng acceleration will further reduce the absolute time, and moreover will prevent possible stabilization of the solution before achieving true convergence.

Finally, an important feature of the present acceleration algorithms is that they are applicable within the whole range of stellar atmospheric models calculated with complete linearization. Therefore, they offer universal, easy-to-use, and robust method for calculating NLTE model atmospheres of hot stars. A model which most sceptics would judge to be too involved for a reasonable application of complete linearization, for instance one with 60 levels and 160 lines taken fully into account in NLTE, may now be calculated to a sufficient accuracy in less than 70 min (the NLTE/L step only; about 2 h if calculated from scratch) on a modern workstation.

Acknowledgements. We thank Bruce Altner for many helpful comments that led to a significant improvement of the manuscript, and for his help with the artwork. We also wish to thank David Hummer, Dimitri Mihalas, George Rybicki, and Steve Shore for helpful discussions and comments on the manuscript.

References

Anderson L.S., 1985, ApJ 298, 848
Anderson L.S., 1987, in: Kalkofen W. (ed.) Numerical Radiative Transfer. Cambridge University Press, Cambridge, p. 163

Auer L.H., 1991, in: Crivellari L., Hubeny I., Hummer D.G. (eds.) Stellar Atmospheres: Beyond Classical Models, NATO ASI Series C 341. Kluwer, Dordrecht, p. 9
Auer L.H., Mihalas D., 1969, ApJ 158, 641
Auer L.H., Mihalas D., 1970, MNRAS 149, 65
Auer L.H., Heasley J.N., Milkey R.W., 1972, Kitt Peak Natl. Obs. Contr. No. 555, Tucson
Borsenberger J., Gros M., 1978, A&AS 31, 291
Broyden C.G., 1965, Math. Comp. 19, 577
Buchler J.R., Auer L.H., 1985, in: Davis J., Hooper C., Lee R., Merts A., Rozsnyai B. (eds.) Proc. 2nd Intern. Conf. and Workshop on Radiat. Properties of Hot Dense Matter. World Scientific, Singapore, p. 48
Carlsson M., 1986, Report No. 33, Uppsala Astronomical Observatory
Dreizler S., Werner K., 1991, in: Crivellari L., Hubeny I., Hummer D.G. (eds.) Stellar Atmospheres: Beyond Classical Models, NATO ASI Series C 341. Kluwer, Dordrecht, p. 155
Frandsen S., 1974, A&A 37, 139
Hamann W.-R., Koesterke L., Wessolowski U., 1991, in: Crivellari L., Hubeny I., Hummer D.G. (eds.) Stellar Atmospheres: Beyond Classical Models, NATO ASI Series C 341. Kluwer, Dordrecht, p. 69
Hubeny I., 1981, A&A 98, 96
Hubeny I., 1986, in: Cowley C.R., Dworetsky M.M., Mégessier C. (eds.) IAU Coll. 90, Upper Main Sequence Stars with Anomalous Abundances. Dordrecht, Reidel, p. 57
Hubeny I., 1988, Comput. Phys. Commun. 52, 103
Hubeny I., 1992, in: Heber U., Jeffery S. (eds.) Atmospheres of Early-type stars, Lecture Notes in Physics. Springer, Berlin, p. 387
Hubeny I., Heap S.R., Altner B., 1991, ApJ 377, L33
Hubeny I., Hummer D.G., Lanz T., 1992, A&A (to be submitted)
Hummer D.G., Mihalas D., 1988, ApJ 331, 794
Kantorovich L.V., 1949, Trudy Mat. Inst. Steklova XXVIII, 104
Kantorovich L.V., Akilov G.P., 1964, Functional Analysis in Normed Spaces. Pergamon Press, New York (translation from Russian)
Kudritzki R.P., 1973, A&A 28, 103
Mihalas D., 1978, Stellar Atmospheres. Freeman, San Francisco
Mihalas D., Heasley J.N., Auer L.H., 1975, A Non-LTE model stellar atmospheres computer program, NCAR-TN/STR-104
Ng K.C., 1974, J. Chem. Phys. 61, 2680
Olson G.L., Auer L.H., Buchler R., 1988, JQSRT 35, 431 (OAB)
Schubert L.K., 1970, Math. Comp. 24, 27
Wait R., 1979, The Numerical Solution of Algebraic Equations. Wiley, Chichester, NY
Werner K., 1986, A&A 161, 177
Werner K., 1987, in: Kalkofen W. (ed.) Numerical Radiative Transfer. Cambridge University Press, Cambridge, p. 67
Werner K., 1989, A&A 226, 265